INTERNATIONAL JOURNAL FOR NUMERICAL METHODS IN FLUIDS
*Int. J. Numer. Meth. Fluids* (2010)
Published online in Wiley InterScience (www.interscience.wiley.com). DOI: 10.1002/fld.2354

# A comparative study of various pressure relaxation closure models for one-dimensional two-material Lagrangian hydrodynamics‡

J. R. Kamm[1,*,†], M. J. Shashkov[2], J. Fung[2], A. K. Harrison[2] and T. R. Canfield[2]

[1]*Computational Shock and Multiphysics Department, Sandia National Laboratories, MS 0378, Albuquerque, NM 87185, U.S.A.*
[2]*Los Alamos National Laboratory, Los Alamos, NM 87545, U.S.A.*

SUMMARY

Lagrangian hydrodynamics of strength-free materials continues to present open issues, even in one dimension. We focus on the problem of closing a system of equations for a two-material cell under the assumption of a single velocity model. There are several existing models and approaches, each possessing different levels of fidelity to the underlying physics and each exhibiting unique features in the computed solutions. We consider three models that take different approaches to breaking the assumption of instantaneous pressure equilibration in the mixed-material cell. The first of these is the well-known method of Tipton, in which a viscosity-like pressure relaxation term is coupled with an otherwise isentropic pressure update to obtain closed-form expressions for the materials' volume fractions and corresponding sub-cell pressures. The second is the physics-inspired, geometry-based pressure relaxation model of Kamm and Shashkov, which is based on an optimization procedure that uses a local, exact Riemann problem. The third model is the unique aspect of this paper, inspired by the work of Delov and Sadchikov and Goncharov and Yanilkin. This sub-scale dynamics approach is motivated by the linearized Riemann problem to initialize volume fraction changes, which are then modified, via the materials' SIEs, to drive the mixed cell toward pressure equilibrium. Each of these approaches is packaged in the framework of a two-step time integration scheme. We compare these multi-material pressure relaxation models, together with corresponding pure-material calculations, on idealized, two-material problems with either ideal-gas or stiffened-gas equations of state. Published in 2010 by John Wiley & Sons, Ltd.

Received 27 January 2010; Revised 31 March 2010; Accepted 1 April 2010

KEY WORDS: Lagrangian hydrodynamics; compressible flow; multi-material flow; pressure relaxation

## 1. INTRODUCTION

Multi-material Lagrangian hydrodynamics of strength-free materials continues to present open issues. We focus on the problem of closing a system of equations for a two-material cell under the assumption of a single velocity model. We do not consider Eulerian-frame multi-material models (e.g. [1, 2]) or the front-tracking approach (e.g. [3]). We assume that the constituents in these multi-material cells are distinct. Such mixed cells arise in Arbitrary Lagrangian–Eulerian (ALE) methods [4] with several materials, where the flow field is projected onto a new mesh during the remap phase, thus rendering a Lagrangian step with a mixed cell unavoidable. We assume that separate material properties are maintained for each material in a multi-material cell, together

*Correspondence to: J. R. Kamm, Computational Shock and Multiphysics Department, Sandia National Laboratories, MS 0378, Albuquerque, NM 87185, U.S.A.
†E-mail: jrkamm@sandia.gov


Contract/grant sponsor: U.S. Department of Energy; contract/grant numbers: DE-AC-94AL85000, DE-AC52-06NA25396

with the materials' volume fractions; these values can be used to reconstruct material interfaces inside a mixed cell. The main challenge is to accurately assign the thermodynamic states of the individual materials' components together with the nodal forces that such a zone generates, despite a lack of detailed information about the velocity distribution within such cells. In particular, for the calculation of both the equation of state (EOS) and the resulting pressure forces, the calculation of the internal energy is of paramount importance.

Of the several existing models for this problem, we consider three. Such models form one part of an overall numerical scheme for solutions to the governing conservation laws. The method of Tipton [5] is an explicit relaxation model. This approach posits a viscosity-like term that is added to the pressure of each material in a mixed cell. By enforcing equality of all materials' augmented pressures and preservation of volume, explicit solutions for the volume changes are obtained, with which the states of the mixed cell constituents are updated. The pressure relaxation method of Kamm and Shashkov [6] is a sub-cell dynamics approach that is based on the instantaneous pressure-equlibration model of Després and Lagoutière [7], in which the materials' change in heat in the mixed cell is assumed equal. Kamm and Shashkov (K&S) replace the instantaneous pressure equilibration with a relaxation procedure based on an optimization problem that uses the solution of a local Riemann problem. Another class of methods, using approximate sub-scale dynamics (SSD), is motivated by the work of Delov and Sadchikov [8] and Goncharov and Yanilkin [9]. One estimates the velocity of the sub-cell interface between materials, which suggests an approximation for the volume change of each material. Using this result, the internal energy for each material is updated separately from its own $p\mathrm{d}V$ equation. This internal energy update contains an energy exchange term between the mixed cell materials, which allows some flexibility in the nature of the pressure relaxation.

This paper is structured as follows. Section 2 contains a brief review of the basic 1D Lagrangian hydrodynamics equations and the predictor–corrector schemes we employ to obtain solutions. In Section 3, we describe the three distinct pressure-relaxation models to be examined: Tipton, K&S, and SSD. A specification of the test problems and the results for this method are provided in Section 4, which also contains comparisons with the results of pure-material calculations. We summarize our findings and conclude in Section 5.

## 2. ONE-DIMENSIONAL LAGRANGIAN HYDRODYNAMICS

The partial differential equations governing the conservation of momentum and internal energy, written in the Lagrangian frame of reference, are (see, e.g. Caramana *et al.* [10]):

$$\rho(\mathrm{d}u/\mathrm{d}t)+\nabla P=0, \tag{1}$$

$$\rho(\mathrm{d}\varepsilon/\mathrm{d}t)+P\nabla\cdot u=0. \tag{2}$$

In these equations, $u$ is the velocity and $P=P(\tau,\varepsilon)$ is the thermodynamic pressure, where $\varepsilon$ is the specific internal energy (SIE) and $\tau$ is the specific volume, which is given by the inverse of the mass density $\rho$ of the fluid. The mass of a fluid parcel is constant, so that $\tau$ is the volume of that parcel divided by its mass. In this section, subscripts denote spatial position and superscripts indicate temporal indexing. In our staggered-mesh discretization, cell-centers (at index $i+\frac{1}{2}$) are associated with cell masses $M_{i+1/2}$, cell volumes $V_{i+1/2}$, and thermodynamic state variables, such as density $\rho_{i+1/2}$, specific volume $\tau_{i+1/2}$, SIE $\varepsilon_{i+1/2}$, pressure $p_{i+1/2}$, and sound speed $c_{s,i+1/2}$. The vertices of cell $i$ are associated with edge positions $x_i$ and $x_{i+1}$, edge velocities $u_i$ and $u_{i+1}$, and node-centered control volume masses $m_i$ and $m_{i+1}$. The volumes are determined from the edge positions, which evolve according to the trajectory equation,

$$\mathrm{d}x_i/\mathrm{d}t=u_i. \tag{3}$$

We assume that we have the necessary information to completely specify all state variables at time $t^n$ and seek to update the solution to time $t^{n+1}\equiv t^n+\delta t$, where $\delta t$ is the timestep. We present two numerical schemes for integrating the pure-material equations. These schemes are stable under

the usual constraints, e.g. on the CFL number. Both are nominally second-order accurate in both space and time for smooth initial conditions and sufficiently short times; the methods invariably degenerate to first order as discontinuous flow features develop. In the first phase of both methods, the assignment of the pressure is based on an adiabatic relation, which is more efficient than an EOS call. The full EOS call in the second phase is retained, to ensure thermodynamic consistency, conservation, and accuracy at the updated time.

### 2.1. A two-step algorithm

An integrator based on a two-step method is used in our implementation of Tipton's and SSD approaches. Here, certain quantities are first updated to the half-timestep level ($H$), and then all flow field quantities are updated to the full timestep ($F$).

| *Half-timestep* | *Full-timestep* | |
|---|---|---|
| | $u_i^{n+1} = u_i^n - \dfrac{\delta t}{m_i}(p_{i+1/2}^{n+1/2} - p_{i-1/2}^{n+1/2})$, | (4) |
| $x_i^{n+1/2} = x_i^n + (\delta t/2)\cdot u_i^n$, | $x_i^{n+1} = x_i^n + (\delta t/2)\cdot(u_i^n + u_i^{n+1})$, | (5) |
| $V_{i+1/2}^{n+1/2} = x_{i+1}^{n+1/2} - x_i^{n+1/2}$, | $V_{i+1/2}^{n+1} = x_{i+1}^{n+1} - x_i^{n+1}$, | (6) |
| $\tau_{i+1/2}^{n+1/2} = V_{i+1/2}^{n+1/2}/M_{i+1/2}$, | $\tau_{i+1/2}^{n+1} = V_{i+1/2}^{n+1}/M_{i+1/2}$, | (7) |
| | $\varepsilon_{i+1/2}^{n+1} = \varepsilon_{i+1/2}^n - p_{i+1/2}^{n+1/2}\delta V_{i+1/2}^{n+1}/M_{i+1/2}$, | (8) |
| $p_{i+1/2}^{n+1/2} = p_{i+1/2}^n - \dfrac{(c_{s,i+1/2}^n)^2}{\tau_{i+1/2}^n}\dfrac{\delta V_{i+1/2}^{n+1/2}}{V_{i+1/2}^n}$, | $p_{i+1/2}^{n+1} = \mathscr{P}(\tau_{i+1/2}^{n+1}, \varepsilon_{i+1/2}^{n+1})$. | (9) |

In (8$F$) and (9$H$), the change in volume is $\delta V_{i+1/2}^{n+j} \equiv V_{i+1/2}^{n+j} - V_{i+1/2}^n$ with $j = 1$ or $\frac{1}{2}$, respectively.

### 2.2. A predictor–corrector algorithm

Our implementation of Kamm and Shashkov's method uses the following predictor–corrector ($P$-$C$) method, which conserves the momentum and total energy.

| *Predictor* | *Corrector* | |
|---|---|---|
| $u_i^{n+1,\star} = u_i^n - \dfrac{\delta t}{m_i}(p_{i+1/2}^n - p_{i-1/2}^n)$, | $u_i^{n+1} = u_i^n - \dfrac{1}{2}\dfrac{\delta t}{m_i}(p_{i+1/2}^n + p_{i+1/2}^{n+1,\star}$ $- p_{i-1/2}^n - p_{i-1/2}^{n+1,\star})$, | (10) |
| $u_i^{n+1/2,\star} = \frac{1}{2}(u_i^n + u_i^{n+1,\star})$, | $u_i^{n+1/2} = \dfrac{1}{2}(u_i^n + u_i^{n+1})$, | (11) |
| $x_i^{n+1,\star} = x_i^n + \delta t\cdot u_i^{n+1/2,\star}$, | $x_i^{n+1} = x_i^n + \delta t\cdot u_i^{n+1/2}$, | (12) |
| $V_{i+1/2}^{n+1,\star} = x_{i+1}^{n+1,\star} - x_i^{n+1,\star}$, | $V_{i+1/2}^{n+1} = x_{i+1}^{n+1} - x_i^{n+1}$, | (13) |
| | $\tau_{i+1/2}^{n+1} = V_{i+1/2}^{n+1}/M_{i+1/2}$, | (14) |
| | $\varepsilon_{i+1/2}^{n+1} = \varepsilon_{i+1/2}^n - \dfrac{1}{2}\dfrac{\delta t}{M_{i+1/2}}(p_{i+1/2}^n + p_{i+1/2}^{n+1,\star})$ $\times(u_{i+1}^{n+1/2} - u_i^{n+1/2})$, | (15) |
| $p_{i+1/2}^{n+1,\star} = p_{i+1/2}^n - \dfrac{(c_{s,i+1/2}^n)^2}{\tau_{i+1/2}^n}\dfrac{\delta V_{i+1/2}^{n+1,\star}}{V_{i+1/2}^n}$, | $p_{i+1/2}^{n+1} = \mathscr{P}(\tau_{i+1/2}^{n+1}, \varepsilon_{i+1/2}^{n+1})$. | (16) |

In (16), the change in volume is $\delta V_{i+1/2}^{n+1,\star} \equiv V_{i+1/2}^{n+1,\star} - V_{i+1/2}^n$.

### *2.3. Artificial viscosity model*

The pressure in these methods (e.g. in $(4F)$, $(8F)$, (10) and (15)) is augmented by an artificial viscosity to provide additional numerical dissipation, e.g. at shock waves. To calculate the artificial viscosity $q^n_{i+1/2}$, the classical linear-plus-quadratic model, active only in compression, is evaluated for right-going waves as:

$$q^n_{i+1/2} = \begin{cases} 0 & \text{if } u^n_{i+1} - u^n_i \geqslant 0, \\ -v_1 \rho^n_{i+1/2} c^n_{s,i+1/2} (u^n_{i+1} - u^n_i) + v_2 \rho^n_{i+1/2} (u^n_{i+1} - u^n_i)^2 & \text{otherwise,} \end{cases} \tag{17}$$

where $v_1$ ($\sim 1$) and $v_2$ ($\sim 0.1$) are the coefficients of the linear and quadratic contributions, respectively, and $\rho^n_{i+1/2} \equiv 1/\tau^n_{i+1/2}$. While more sophisticated artificial viscosity models certainly exist (see, e.g. [11]), the simple model of (17) is sufficient for demonstration purposes.

## 3. TWO-MATERIAL PRESSURE RELAXATION MODELS

In this section, we describe three different closure models that relax the constituent pressures to equilibrium in a mixed cell. That is, given an initial state with a discrepancy between the pressures of material 1 and material 2, we seek a model with which to update the individual materials' pressures such that the difference between these values approaches zero as time increases, in the absence of any external forcing.

Conceptually, there is a relaxation operator $\mathscr{R}$ that takes as input the thermodynamic states of the constituent materials at time $t^n$ together with values for the overall specific volume and SIE at time $t^{n+1}$. This operator returns the states of the individual materials updated to time $t^{n+1}$ and an estimate of an updated common cell pressure:

$$\mathscr{R}(\tau^n_1, \varepsilon^n_1, \tau^n_2, \varepsilon^n_2; \tau^{n+1}, \varepsilon^{n+1}) = [\tau^{n+1}_1, \varepsilon^{n+1}_1, \tau^{n+1}_2, \varepsilon^{n+1}_2; p^{n+1}]. \tag{18}$$

We now describe different approaches that, in effect, model the relaxation operator $\mathscr{R}$.

### *3.1. Tipton's model*

For Tipton's pressure relaxation method [5] with two materials, the pressure of each material is first updated with an adiabatic approximation (as in $(9H)$), which includes that material's unknown volume change, $\delta V^{n+1/2}_k$:

$$p^{n+1/2}_k = p^n_k - [(c^n_{s,k})^2/\tau^n_k](\delta V^{n+1/2}_k / V^n_k), \tag{19}$$

where here and in the following, subscripts indicate the material, and not the cell index. A third unknown is the overall half-timestep pressure, $p^{n+1/2}$, which is identical for all the materials. It is assumed to equal the sum of each material's pressure and a unique relaxation term:

$$p^{n+1/2} = p^{n+1/2}_k + R^{n+1/2}_k, \quad k = 1, 2. \tag{20}$$

The second term on the RHS of (20) is posited to have the following form:

$$R^{n+1/2}_k = -(c^n_{s,k}/\tau^n_k)(L^n/\delta t)(\delta V^{n+1/2}_k / V^n_k), \tag{21}$$

where $L^n$ is a characteristic length for the mixed cell (e.g. the overall cell size). The above three relations can be combined into the following equation, for $k = 1, 2$:

$$p^{n+1/2} = p^n_k - \tilde{B}^n_k (\delta V^{n+1/2}_k / V^n_k) \quad \text{where } \tilde{B}^n_k \equiv \rho^n_i [(c^n_{s,k})^2/\tau^n_k][1 + L^n/(c^n_{s,k}\delta t)]. \tag{22}$$

To close this model, one enforces that the sum of the (unknown) volume changes of all materials equals the overall volume change of the mixed cell, $V^{n+1/2}$, which is known from the half-timestep update (using the expression in $(6H)$ as $\delta V^{n+1/2}$):

$$\delta V_1^{n+1/2} + \delta V_2^{n+1/2} = \delta V^{n+1/2}. \tag{23}$$

The equalities in (22) and (23) form a linear system of equations in the unknowns $\delta V_1^{n+1/2}$, $\delta V_2^{n+1/2}$, and $p^{n+1/2}$. This system has the closed-form solution, for $k=1,2$:

$$\delta V_k^{n+1/2} = \frac{V_k^n}{\tilde{B}_k^n}[(p_k^n - \bar{p}^n) + \bar{B}^n(\delta V^{n+1/2}/V^n)], \quad p^{n+1/2} = \bar{p}^n - \bar{B}^n(\delta V^{n+1/2}/V^n), \tag{24}$$

where the barred values are the volume-fraction-averaged quantities given by

$$\bar{p}^n \equiv \sum_{k=1}^{2}\left(\frac{f_k^n p_k^n}{\tilde{B}_k^n}\right) \Bigg/ \sum_{k=1}^{2}\left(\frac{f_k^n}{\tilde{B}_k^n}\right) \quad \text{and} \quad \bar{B}^n \equiv \left[\sum_{k=1}^{2}\left(\frac{f_k^n}{\tilde{B}_k^n}\right)\right]^{-1}, \tag{25}$$

with $f_k$ as the volume fraction of the $k$th material. In (24), two mechanisms contribute to $\delta V_k^{n+1/2}$: (i) the difference between the $k$th material pressure and the 'averaged' pressure given by $\bar{p}^n$, and (ii) the overall volume change of the cell. The $k$th material volume is related to the overall cell volume by the volume fraction, i.e. $V_k = f_k V$. This leads to the relation:

$$\delta f_k^{n+1/2} = f_k^n[(p_k^n - \bar{p}^n)/\tilde{B}_k^n] + f_k^n[(\bar{B}^n/\tilde{B}_k^n) - 1](\delta V^{n+1/2}/V^n). \tag{26}$$

To update to $t^{n+1}$, we invoke the final assumption, namely, that the individual materials' volume changes at $t^{n+1} = t^n + \delta t = t^n + 2\cdot(\delta t/2)$ equal twice the half-timestep values:

$$\delta f_k^{n+1} = 2\delta f_k^{n+1/2} \quad \text{and} \quad f_k^{n+1} = f_k^n + \delta f_k^{n+1}. \tag{27}$$

The materials' volumes, volume changes, and densities are evaluated as:

$$V_k^{n+1} = f_k^{n+1} V^{n+1}, \quad \delta V_k^{n+1} = V_k^{n+1} - V_k^n \quad \text{and} \quad \rho_k^{n+1} = M_k / V_k^{n+1}. \tag{28}$$

As in the overall cell case, the SIE for each material is obtained from the updated $p\,dV$ work:

$$\varepsilon_k^{n+1} = \varepsilon_k^n - p^{n+1/2}\delta V_k^{n+1}/M_k. \tag{29}$$

Finally, the individual pressures are evaluated consistently with full EOS calls:

$$p_k^{n+1} = \mathscr{P}_k(\tau_k^{n+1}, \varepsilon_k^{n+1}). \tag{30}$$

### *3.2. Kamm and Shashkov's model*

The approach of Kamm and Shashkov (K&S) models the sub-cell dynamics of the mixed cell through the local Riemann problem in the multi-material cell over one timestep. The following description is for a single timestep; a full explanation for a two-step time integrator is given in [6]. Let the mixed cell be identified by the index $i_{\text{mix}}$. The interface between the materials is determined by the local volume fraction of, say, material 1, given by $f_1$:

$$x_{\text{intfc}}^n = x_{i_{\text{mix}}}^n + f_1(x_{i_{\text{mix}}+1}^n - x_{i_{\text{mix}}}^n) \in [x_{i_{\text{mix}}}^n, x_{i_{\text{mix}}+1}^n]. \tag{31}$$

The two states in this cell at $t^n$ are given by:

$$(\rho, \varepsilon, p, u) = \begin{cases} (\rho_1, \varepsilon_1, p_1, u_1) & \text{if } x_{i_{\text{mix}}}^n < x < x_{\text{intfc}}^n, \\ (\rho_2, \varepsilon_2, p_2, u_2) & \text{if } x_{\text{intfc}}^n < x < x_{i_{\text{mix}}+1}^n. \end{cases} \tag{32}$$

The obvious and the simplest choice for the materials' velocities in 1D is

$$u_1 = u_{i_{\text{mix}}} \quad \text{and} \quad u_2 = u_{i_{\text{mix}}+1}. \tag{33}$$

The exact solution to this one-cell Riemann problem at time $t^{n+1}$ can be computed for polytropic gases [12], for stiffened gases [13], and for more general EOS [14].

The key assumption of the K&S approach is as follows: obtain a single updated (i.e. at $t^{n+1}$) pressure for each material in the mixed cell that minimizes the discrepancy between that value and the pressure given by the Riemann problem solution in that material. This relation is expressed mathematically in the mixed cell as the following optimization requirement:

$$\min_{\{\tau_1^{n+1},\varepsilon_1^{n+1},\tau_2^{n+1},\varepsilon_2^{n+1}\}} (\|p_1^{n+1}-p_1^{\mathrm{RP}}\|^2+\|p_2^{n+1}-p_2^{\mathrm{RP}}\|^2). \tag{34}$$

This problem is subject to the following constraints:

$$\mathscr{F}_1 \equiv c_1\tau_1^{n+1}+c_2\tau_2^{n+1}-\tau^{n+1}=0, \tag{35}$$

$$\mathscr{F}_2 \equiv c_1\varepsilon_1^{n+1}+c_2\varepsilon_2^{n+1}-\varepsilon^{n+1}=0, \tag{36}$$

$$\mathscr{F}_3 \equiv \varepsilon_1^{n+1}-\varepsilon_1^n+P_1(\tau_1^{n+1}-\tau_1^n)-[\varepsilon_2^{n+1}-\varepsilon_2^n+P_2(\tau_2^{n+1}-\tau_2^n)]=0, \tag{37}$$

where $c_k$ is the mass fraction of material $k$. These equations represent, respectively, the conservation of mass, balance of internal energy, and equality of the change of heat. The pressures in (37) are written as $P_k$ to indicate the freedom to specify $p_k^n$, $p_k^{n+1}$, or $\frac{1}{2}(p_k^n+p_k^{n+1})$ for this value, as discussed by Kamm and Shashkov [6]. In (34), $p_k^{\mathrm{RP}}$ is the pressure, in material $k$, related to the solution of the Riemann problem. Reference [6] gives the details on how to obtain solutions to this optimization problem, together with the motivation as to why this approach can lead to pressure relaxation.

### *3.3. Sub-scale dynamics model*

An alternate, approximate SSD approach is inspired by the work of Delov and Sadchikov [8] and Goncharov and Yanilkin [9]. In 1D, the velocity of the sub-cell interface between the materials, $u_{\mathrm{intfc}}$,[§] is given by the linearized Riemann-solver approximation as:

$$u_{\mathrm{intfc}} = \frac{\rho_1 c_{s,1} u_1^- + \rho_2 c_{s,2} u_2^+ + (p_1 - p_2)}{\rho_1 c_{s,1} + \rho_2 c_{s,2}}, \tag{38}$$

where we have superscripted the flow velocities with '$-$' and '$+$' to emphasize that these values are to the immediate left and right of the interface, respectively. Assuming that the velocity varies linearly within the cell (so that it is continuous at the interface), it is easily shown that

$$u_1^- = u_2^+ = f_2 u_1 + f_1 u_2, \tag{39}$$

where the unsuperscripted velocities on the RHS of (39) are the values at the cell edges, i.e. $u_1 = u_{i_{\mathrm{mix}}}$ and $u_2 = u_{i_{\mathrm{mix}}+1}$. We substitute these quantities into (38) and simplify to obtain

$$u_{\mathrm{intfc}} = f_2 u_1 + f_1 u_2 + \frac{p_1 - p_2}{\rho_1 c_{s,1} + \rho_2 c_{s,2}}. \tag{40}$$

The corresponding volume changes of the materials in a mixed cell are given by:

$$\delta V_1 = (u_{\mathrm{intfc}} - u_1)\delta t, \quad \delta V_2 = (u_2 - u_{\mathrm{intfc}})\delta t. \tag{41}$$

[§]The quantity $u_{\mathrm{intfc}}$ is the velocity *of* the interface, and not the flow velocity *at* the interface.

Substituting (40) into (41) provides the following expressions for the volume changes:

$$\delta V_1 = f_1 \delta V + \frac{p_1 - p_2}{\rho_1 c_{s,1} + \rho_2 c_{s,2}} \delta t, \quad \delta V_2 = f_2 \delta V - \frac{p_1 - p_2}{\rho_1 c_{s,1} + \rho_2 c_{s,2}} \delta t, \tag{42}$$

where the volume change of the entire cell over the timestep, $\delta V$, is substituted for $(u_2 - u_1)\delta t$.

Prompted by this result, we write the mixed-cell predictor volume update as

$$\delta V_1^{n+1/2} = f_1^n \delta V^{n+1/2} + \frac{p_1^n - p_2^n}{\kappa_1^n + \kappa_2^n}(\delta t/2), \quad \delta V_2^{n+1/2} = f_2^n \delta V^{n+1/2} - \frac{p_1^n - p_2^n}{\kappa_1^n + \kappa_2^n}(\delta t/2), \tag{43}$$

where $\kappa_k^n = \rho_k^n c_{s,k}^n$, $k = 1, 2$. We update the materials' volumes, volume fractions, and pressures:

$$V_k^{n+1/2} = V_k^n + \delta V_k^{n+1/2}, \quad f_k^{n+1/2} = \frac{V_k^{n+1/2}}{V^{n+1/2}}, \quad p_k^{n+1/2} = p_k^n - \frac{(c_{s,k}^n)^2}{\tau_k^n} \frac{\delta V_k^{n+1/2}}{V_k^n}. \tag{44}$$

The overall cell pressure is the volume-fraction weighted sum of the individual pressures.

In the corrector step, the velocities are computed from $(4F)$ using this overall pressure. The values at $t^{n+1}$ of the overall cell positions and volume are calculated as in $(5F)$, $(6F)$. The individual volume changes of the materials are assigned similar to (43), but with volume fractions and pressures from (44) and the full timestep, $\delta t$. The corrector volumes and volume fractions are calculated in a manner similar to (44); the values of $V_k^{n+1}$ are used to update the specific volumes $\tau_k^{n+1}$ as in (7). Motivated by the assumption that each material obeys its own isentropic relation, we update the individual SIEs as

$$m_1 d\varepsilon_1 = -p_1^{n+1/2} f_1^{n+1/2} \delta V^{n+1} - p_{1,2}^{\star,n+1/2} \frac{p_1^{n+1/2} - p_2^{n+1/2}}{\kappa_1^{n+1/2} + \kappa_2^{n+1/2}} \delta t, \tag{45}$$

$$m_2 d\varepsilon_2 = -p_2^{n+1/2} f_2^{n+1/2} \delta V^{n+1} + p_{1,2}^{\star,n+1/2} \frac{p_1^{n+1/2} - p_2^{n+1/2}}{\kappa_1^{n+1/2} + \kappa_2^{n+1/2}} \delta t. \tag{46}$$

Here, $p_{1,2}^{\star,n+1/2}$ represents an interfacial pressure term, which we model with the star-state pressure of the standard acoustic Riemann problem [15]:

$$p_{1,2}^{\star,n+1/2} = \frac{\kappa_2^{n+1/2} p_1^{n+1/2} + \kappa_1^{n+1/2} p_2^{n+1/2}}{\kappa_1^{n+1/2} + \kappa_2^{n+1/2}} - \frac{\kappa_1^{n+1/2} \kappa_2^{n+1/2}}{\kappa_1^{n+1/2} + \kappa_2^{n+1/2}} (u_{i_{\text{mix}}+1}^{n+1} - u_{i_{\text{mix}}}^{n+1}). \tag{47}$$

To complete the corrector step, the individual materials' pressures are updated with calls to the respective equations of state, as in (30).

The model in (45)–(47) differs significantly from Tipton's method: each material's SIE is updated through its own pressure, and the second addends on the RHS of (45), (46) can be interpreted as *de facto* 'energy exchange' terms. There is significant flexibility in specifying these quantities; Equations (45)–(47) are just one possible model. Alternatively, for example, one could enforce the positivity of each material's SIE.

## 4. TEST PROBLEMS AND RESULTS

We consider two different test problems from the compressible flow literature with which to evaluate the methods described above. We consider only problems with exact solutions, so that we can compare, qualitatively and quantitatively, the different methods' errors.

In the mixed-cell test problems, the mesh has $N_x$ zones, each of initial dimension $1/(N_x + 1)$, with the exception of a single multi-material zone, which is of initial width $2/(N_x + 1)$. In that

multi-material zone, the mass and volume fractions are assigned to be consistent with the initial conditions, with the initial material interface located at the geometric center of the cell. We compare the results with a pure-material calculation, i.e. with *no* mixed cell, in which all cells are initially the same width; these calculations contain one more cell than the multi-material calculations: the multi-material zone is split into two equal-sized pure-material zones for a total of $N_x+1$ zones, each of width $1/(N_x+1)$.[¶] Insofar as all models are different approximations to the underlying continuous equations, it is plausible that the numerical solutions of the multi-material model could be closer to the exact solution than the pure Lagrangian calculations. All problems were run with the same value of CFL constant, equal to 0.5.[‖] In the K&S results, an absolute $L_1$ convergence tolerance for Newton's method of at least $10^{-10}$ was imposed in the modified Sod shock tube problem of Section 4.1 and $10^{-7}$ in the dimensional water–air shock tube problem of Section 4.2. We provide snapshots of the computed and exact flow fields at the final time together with the time-histories of the material properties in the multi-material cell or, in the pure-material calculation, adjacent to the interface.

### *4.1. The modified Sod shock tube*

We consider the modified shock tube problem variant introduced by Barlow [16] (see also [5]), with the following non-dimensional initial conditions and a final time of $t_{\text{final}}=0.2$:

$$(\gamma,\rho,\varepsilon,p,u)=\begin{cases}(2,1,2,2,0) & \text{if } 0<x<0.5,\\ (1.4,0.125,2,0.1,0) & \text{if } 0.5<x<1,\end{cases} \tag{48}$$

where $p=(\gamma-1)\rho\varepsilon$. The mixed cell initially contains both of these distinct states.

Figure 1 contains the snapshots of the results at the final time for all the methods. The pressure results are quite similar, whereas the Tipton method results have a slightly less accurate rarefaction tail, greater density undershoot and more significant SIE overshoot at the contact. The SSD approach is notable both for the well-behaved density contact and the modest SIE overshoot at the contact. The K&S results fall somewhere between those results. All the methods are found to converge at very nearly first order in the $L_1$ norm for this problem.

The plots of the time-histories for all methods are shown in Figure 2. The nature of the pressure-equilibration varies, with the SSD calculation equilibrating the quickest. The final values of density and SIE differ slightly among the methods, with the SSD final values being the best of the multi-material methods, followed by K&S, and then Tipton. The SSD time-histories are perhaps closest to those of the pure-material calculation.

### *4.2. Water–air shock tube*

The water–air shock tube is a standard problem for multi-material compressible flow [17]. It tests inherently compressible flow features, uses a slightly more complicated and stiffer EOS than the standared polytropic gas, and possesses a directly computable solution. The thermodynamic properties of water in this problem are given by the stiffened-gas EOS:

$$p=(\gamma-1)\rho\varepsilon-\gamma p_\infty. \tag{49}$$

[¶]It is not necessary that these methods be used either with mixed cells that are larger than the non-mixed cells or with the interface in the geometric middle of the mixed cell. We have set up the test problems in the manner described above in order to compare, as closely as possible, to the corresponding pure-material calculations.

[‖]Kamm and Shashkov [6] state that, for the modified Sod problem, the results appear to be insensitive to the CFL values less than or equal to 0.5; at higher values of the CFL number, numerical instabilities were seen.

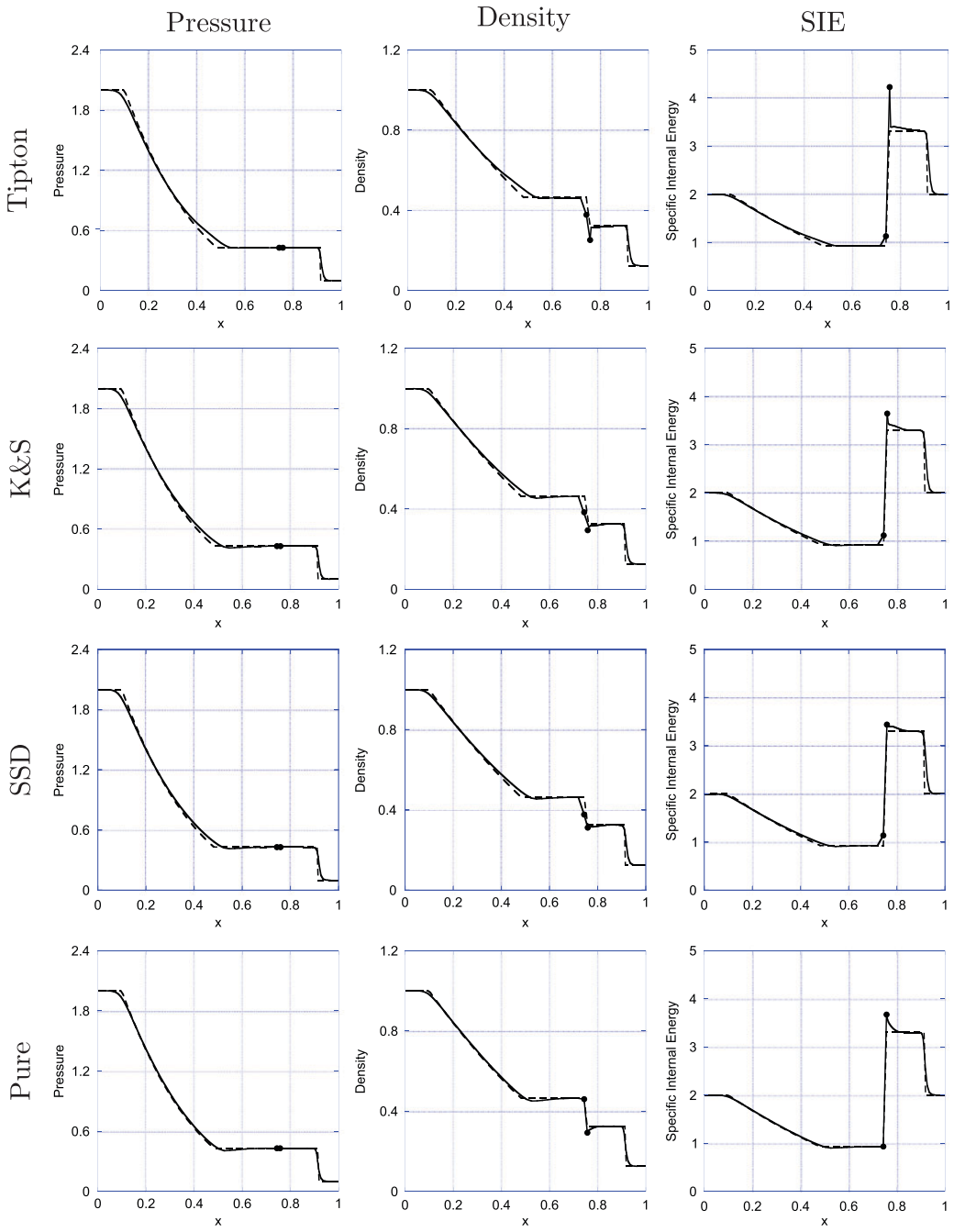


Figure 1. Results for the modified Sod shock tube problem on $[0, 1]$ at $t = 0.2$ for (from left to right) pressure, mass density, and SIE, with (from top to bottom) Tipton's method (99 zones), the K&S method (99 zones), the SSD method (99 zones), and the pure-cell calculation (100 zones). The computed results are the solid line, the exact solution is the dashed line, and the values corresponding to the individual materials in the mixed cell are indicated with the bullets.

The initial conditions for the water–air shock tube problem, in mks units, are:

$$(\gamma, p_\infty, \rho, \varepsilon, p, u) = \begin{cases} (4.4, 6\times10^8, 10^3, 1.07\times10^6, 10^9, 0) & \text{if } 0<x<0.7, \\ (1.4, 0, 50, 5\times10^4, 10^6, 0) & \text{if } 0.7<x<1, \end{cases} \tag{50}$$

with a final time of $t_{\text{final}} = 2.2\times10^{-4}$ s. The multi-material cell is initially centered at $x = 0.7$.

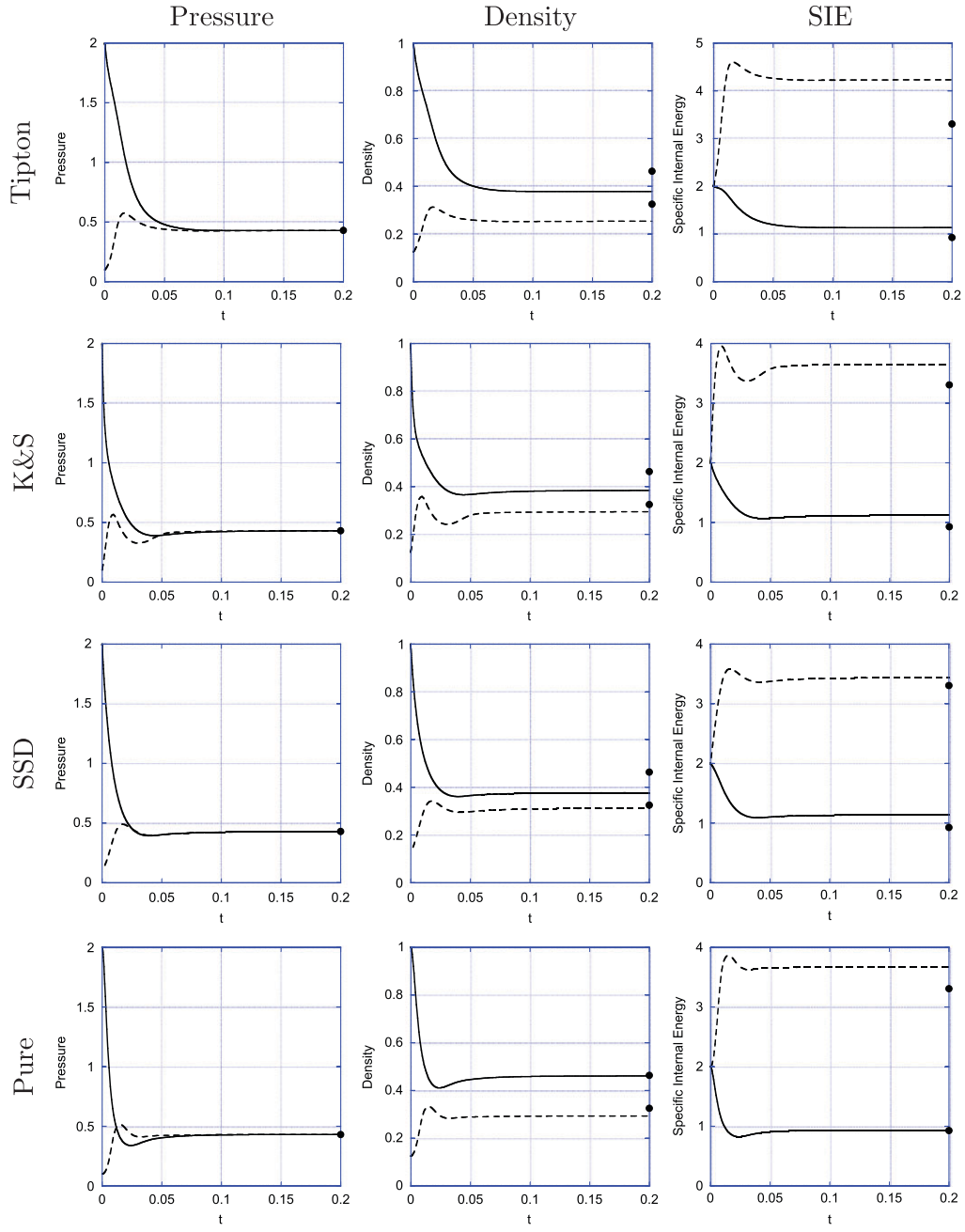


Figure 2. Time-history plots for the modified Sod shock tube problem of the (from left to right) pressure, the mass density, and SIE, with (from top to bottom) Tipton's method (99 zones), the K&S method (99 zones), the SSD method (99 zones), and the pure-cell calculation (100 zones). The top three rows are for two materials in the mixed cell; the bottom row is for the cells immediately adjacent to the material interface. The solid line indicates the left material (material 1), the dotted line represents the right material (material 2), and the bullets represent the exact solution at the final time.

Figure 3 shows the final-time snapshots for all the methods. The pressure snapshots are similar, with the exception of a slight 'bump' in the pressure at the tail of the rarefaction for Tipton. The SSD result has the smallest density undershoot at the contact, whereas the K&S result has, next to the pure-material calculation, the best SIE behavior at the contact. As in the previous problem, all the results are found to converge at very nearly first order in the $L_1$ norm.

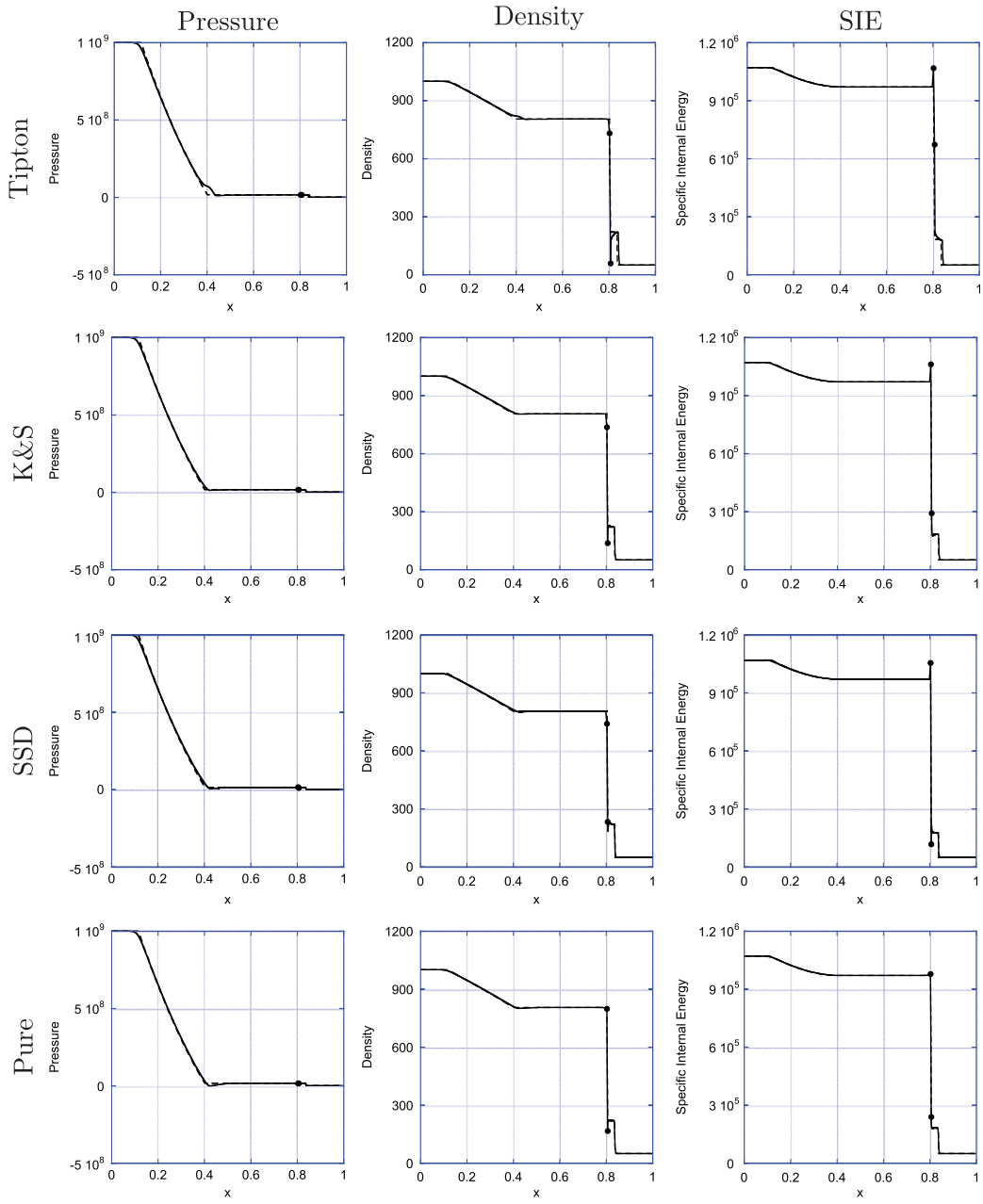


Figure 3. Results for the water–air shock tube problem on $[0, 1]$ at $t = 2.2 \times 10^{-4}$ for (from left to right) pressure, mass density, and SIE with (from top to bottom) Tipton's method (249 zones), the K&S method (249 zones), the SSD method (249 zones), and the pure-cell calculation (250 zones). The computed results are the solid line, the exact solution is the dashed line, and the values corresponding to the individual materials in the mixed cell are indicated with the bullets.

The time-histories for all the methods are shown in Figure 4. The K&S method equilibrates monotonically in all quantities, the SSD approach undershoots slightly in material 1 pressure and density, and Tipton exhibits the greatest under- and overshoots (including negative pressures, as in the pure-material case). All calculations, except Tipton, are monotonic in material 2 (air). The pure material final values are the closest to the exact values, followed by SSD, K&S, and Tipton, although it is unclear if the SSD results have completely equilibrated.

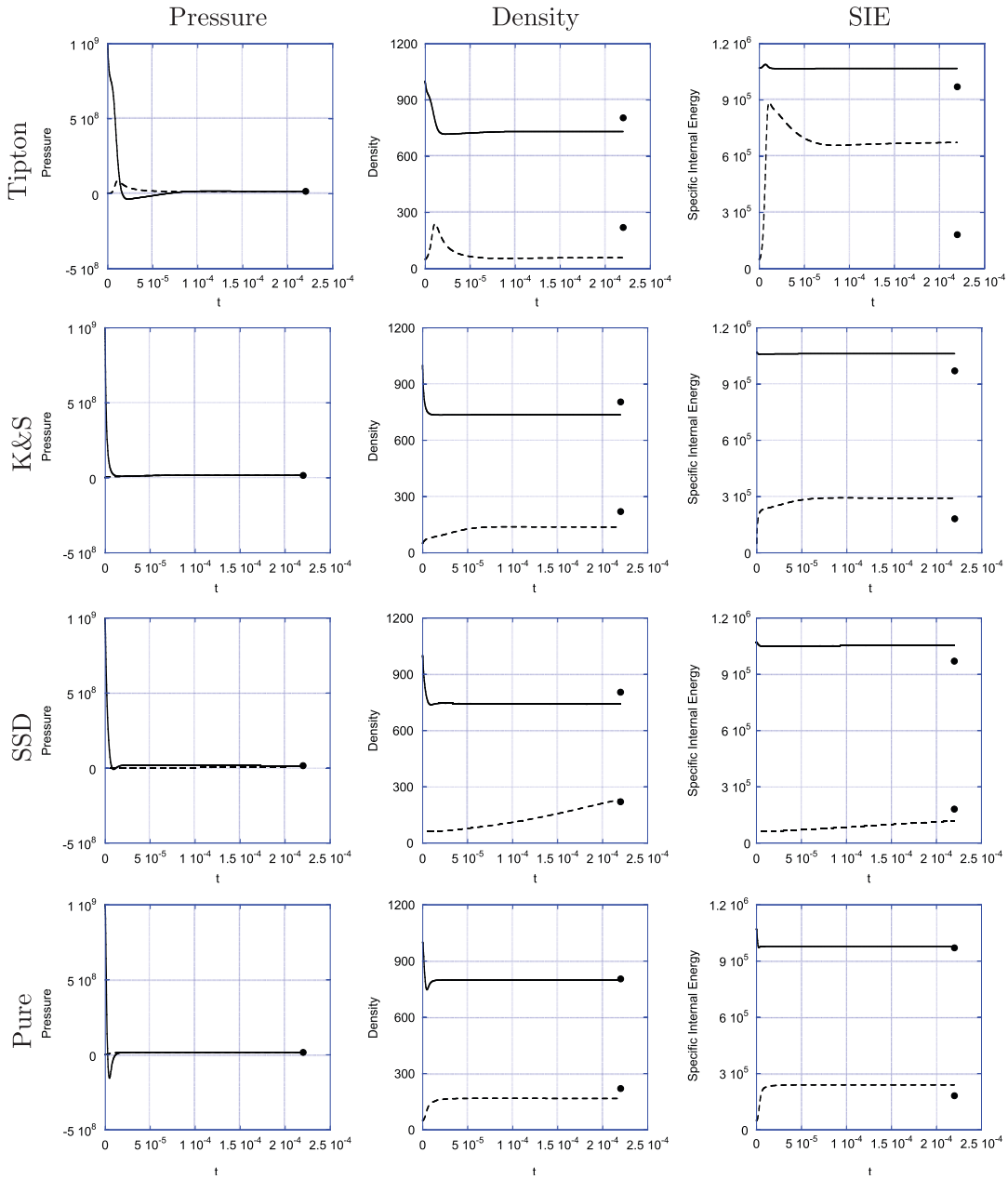


Figure 4. Time-history plots for the water–air shock tube problem on $[0, 1]$ for (from left to right) pressure, mass density, and SIE with (from top to bottom) Tipton's method (249 zones), the K&S method (249 zones), the SSD method (249 zones), and the pure-cell calculation (250 zones). The solid line indicates the left material (material 1), the dotted line represents the right material (material 2), and the bullets represent the exact solution at the final time.

## 5. SUMMARY AND CONCLUSIONS

We have addressed the problem of closing the system of equations for a two-material cell under the single velocity, single pressure assumption in one-dimensional Lagrangian hydrodynamics. The materials in the mixed cells are treated as distinct, presenting the problem of how to assign the thermodynamic states of the individual materials together with the nodal forces that this zone generates. We considered three approaches. Tipton's method [5] is an explicit relaxation scheme

with a viscosity-like term added to the pressure of each material, which uses the equality of all materials' augmented pressures to determine the states of the mixed cell constituents. Kamm and Shashkov [6] base their sub-cell model on that of Després and Lagoutière [7], but break the assumption of instantaneous pressure equilibration with a sub-cell dynamics model that uses an optimization approach related to a local Riemann problem. The unique contribution of this work is the SSD approach, motivated by the work of Delov and Sadchikov [8] and Goncharov and Yanilkin [9], which uses the individual materials' energy equations, mediated by an energy exchange term. These methods were implemented in two-step integration schemes that conserve the momentum and total energy.

The results for two test problems are shown and compared with exact solutions and corresponding pure-material calculations (with no mixed cell). The mixed-cell solutions exhibit slight over- or undershoots in SIE and density (more noticeable in the water–air shock problem). Overall, the SSD results are closest to the exact solution snapshots, whereas the K&S solutions are closer to the pure-material snapshots than those of Tipton's method. On both problems, mixed cell pressure histories for all the methods evolve smoothly—but not necessarily monotonically—toward equilibrium. In the other fields, for modified Sod the oscillations in the time-histories for SSD and Tipton are comparable and less than those of K&S, whereas the water-air shock tube shows the SSD and K&S results to be comparably monotonic.

The SSD results show sufficient promise to warrant further development. There are other 1D test problems on which these methods should be evaluated, including higher Mach number flows and cases with very small initial volume fractions. We are devising methods based on the SSD approach for multi-material cells in higher dimensions; the 2D Lagrangian hydrodynamics version has been tested and will soon be submitted for publication (Harrison *et al*., in preparation, 2010).

## ACKNOWLEDGEMENTS

This work was performed under the auspices of the US Department of Energy's National Nuclear Security Administration by Sandia National Laboratories, a multi-program laboratory operated by Sandia Corporation, a wholly owned subsidiary of Lockheed Martin company, under contract DE-AC-94AL85000, and by Los Alamos National Security, LLC, at Los Alamos National Laboratory, under contract DE-AC52-06NA25396. The authors gratefully acknowledge the partial support of the US DOE NNSA's Advanced Simulation and Computing (ASC) Program and the partial support of the US DOE Office of Science Advanced Scientific Computing Research (ASCR) Program in Applied Mathematics Research. The authors thank A. Barlow, Yu. Bondarenko, D. Burton, B. Després, P.-H. Maire, L. Margolin, W. Rider, and Yu. Yanilkin for numerous stimulating discussions on these topics, and thank the anonymous reviewers for their insightful comments and helpful suggestions.

## REFERENCES

1. Colella P, Glaz HM, Ferguson ME. Multifluid algorithms for Eulerian finite difference methods. *Preprint*, 1996.
2. Miller GH, Puckett EG. A high-order Godunov method for multiple condensed phases. *Journal of Computational Physics* 1996; **128**:134–164.
3. Glimm J, Grove JW, Li XL, Shyue K-M, Zeng Y, Zhang Q. Three-dimensional front tracking. *SIAM Journal on Scientific Computing* 1998; **19**:703–727.
4. Hirt CW, Amsden AA, Cook JL. An arbitrary Lagrangian–Eulerian computing method for all flow speeds. *Journal of Computational Physics* 1974; **14**:227–253.
5. Shashkov MJ. Closure models for multimaterial cells in arbitrary Lagrangian–Eulerian hydrocodes. *International Journal for Numerical Methods in Fluids* 2007; **56**:1497–1504.
6. Kamm JR, Shashkov MJ. A pressure relaxation closure model for one-dimensional, two-material Lagrangian hydrodynamics based on the Riemann problem. *Communications in Computational Physics* 2010; **7**:927–976.
7. Després B, Lagoutière F. Numerical resolution of a two-component compressible fluid model with interfaces. *Progress in Computational Fluid Dynamics* 2007; **7**:295–310.
8. Delov VI, Sadchikov VV. Comparison of several models for computation of thermodynamical parameters for heterogeneous Lagrangian cells. *VANT* (*Mathematical Modeling of Physical Processes*) 2005; **1**:57–70 (in Russian).
9. Goncharov EA, Yanilkin Yu. New method for computations of thermodynamical states of the materials in the mixed cells. *VANT* (*Mathematical Modeling of Physical Processes*) 2004; **3**:16–30 (in Russian).
10. Caramana EJ, Burton DE, Shashkov MJ, Whalen PP. The construction of compatible hydrodynamics algorithms utilizing conservation of total energy. *Journal of Computational Physics* 1999; **146**:227–262.

11. Campbell J, Shashkov M. A tensor artificial viscosity using a mimetic finite difference algorithm. *Journal of Computational Physics* 2001; **172**:739–765.
12. Gottlieb JJ, Groth CPT. Assessment of Riemann solvers for unsteady one-dimensional inviscid flows of perfect gases. *Journal of Computational Physics* 1988; **78**:437–458.
13. Plohr B. Shockless acceleration of thin plates modeled by a tracked random choice method. *AIAA Journal* 1988; **26**:470–478.
14. Colella P, Glaz HM. Efficient solution algorithm for the Riemann problem for real gases. *Journal of Computational Physics* 1985; **59**:264–289.
15. LeVeque R. *Finite Volume Methods for Hyperbolic Problems*. Cambridge University Press: Cambridge, 2002.
16. Barlow A. A new Lagrangian scheme for multimaterial cells. *Proceedings of European Congress on Computational Methods in Applied Sciences and Engineering, ECCOMAS Computational Fluid Dynamics Conference*, Swansea, Wales, U.K., 4–7 September 2001; 235–294.
17. Saurel R, Abgrall R. A multiphase Godunov method for compressible multifluid and multiphase flows. *Journal of Computational Physics* 1999; **150**:425–467.